Short communication

Cellulose-nanofiber/polygalacturonic acid coatings with high oxygen barrier and targeted release properties

Susanne L. Mølgaard [a], Marielle Henriksson [d], Marité Cárdenas [a,c,*], Anna J. Svagan [b,*]

[a] University of Copenhagen, Department of Chemistry, Universitetsparken 5, DK-2100 Copenhagen, Denmark
[b] University of Copenhagen, Inst. for Food Research, Rolighedsvej 30, DK-1958 Frederiksberg C, Denmark
[c] Biomedical Laboratory Science, Faculty of Health and Society, Malmö University, SE-205 06 Malmö, Sweden
[d] SP Technical Research Institute of Sweden, Department of Wood Technology, PO Box 5609, SE-114 86 Stockholm, Sweden

ARTICLE INFO

ABSTRACT

A bio-inspired coating consisting of pectin (polygalacturonic acid) and cationic cellulose nanofibers were successfully produced by the layer-by-layer method. The build-up and the morphology of the resulting coatings were studied with spectroscopic ellipsometry and atomic force microscopy, respectively. The coating was able to survive the exposure of a simulated gastric fluid, but was partially degraded upon exposure to pectinase enzyme, which simulate the action of the microbial symbionts present in the human colon. Prior to exposure, the oxygen permeability coefficient of the coating ($0.033 \, \mathrm{ml \, (STP) \, mm \, m^{-2} \, day^{-1} \, atm^{-1}}$ at $23\,^\circ\mathrm{C}$ and 20% RH) was in the same order of magnitude as for ethylene vinyl alcohol films (0.001–$0.01 \, \mathrm{ml \, (STP) \, mm \, m^{-2} \, day^{-1} \, atm^{-1}}$). However, after exposure to the mimicked gastrointestinal (GI) tract conditions, the contribution of coating to the overall barrier properties was not measurable.

1. Introduction

The Layer-by-layer (LbL) technique has been extensively studied over the past two decades due to its very precise way of controlling film structure and composition at the nanoscale. Advantages of such a bottom-up technique over other available processing techniques, e.g. solvent casting, have previously been demonstrated and discussed for many systems (Svagan et al., 2012; Westwood et al., 2011, 2013). Using this relatively simple technique, a whole range of thin multilayer films or coatings have been prepared, exhibiting unique multifunctional properties such as ultra-high gas barrier properties (Priolo, Gamboa, Holder, & Grunlan, 2010), antimicrobial (Dubas, Kumlangdudsana, & Potiyaraj, 2006), flame retardant (Li et al., 2010), and sensing properties (Kim, Kim, & Shiratori, 2004). The LbL technique consists of alternating dipping and rinsing steps (depicted in Scheme 1a) in dilute solutions of oppositely charged polymers/colloids. After each dipping step a thin layer is deposited, and the thickness of the adsorbed layer can be altered by processing parameters such as temperature (Sukhishvili, 2005) and pH (Wood, Boedicker, Lynn, & Hammond, 2005).

Recently, much attention has been directed to bio-based polymers as sustainable alternatives to man-made polymers in various fields of application including food packaging. The polysaccharide that probably has gained most attention is cellulose nanofibers (NFC), also denoted microfibrillated cellulose or nanofibrillated cellulose. This is mainly due to properties such as mechanical strength and stiffness (crystal modulus) approaching that of Kevlar (Saito, Kuramae, Wohlert, Berglund, & Isogai, 2013) and Steel (Eichhorn et al., 2010), respectively. In addition, NFC are non-toxic and neat NFC based films exhibit oxygen barrier properties (0% RH, $23\,^\circ\mathrm{C}$) that are two orders of magnitude better than ethylene vinyl alcohol (EVOH), typically used in high barrier applications (Aulin, Gallstedt, & Lindstrom, 2010). Natural cellulose nanofibers are only weakly charged, but by chemical modification it is possible to prepare both anionically and cationically charged cellulose nanofibers, making them more suitable candidates in LbL deposition.

Pectin is a complex anionically charged polysaccharide that is naturally present in plant cell walls. Pectin is a large polysaccharide consisting mainly of linear chains of α-($1 \rightarrow 4$)-linked D-galacturonic acid (homogalacturonan) in addition to bulky and highly branched segments (Rhamnogalacturonan I) (Buchanan,
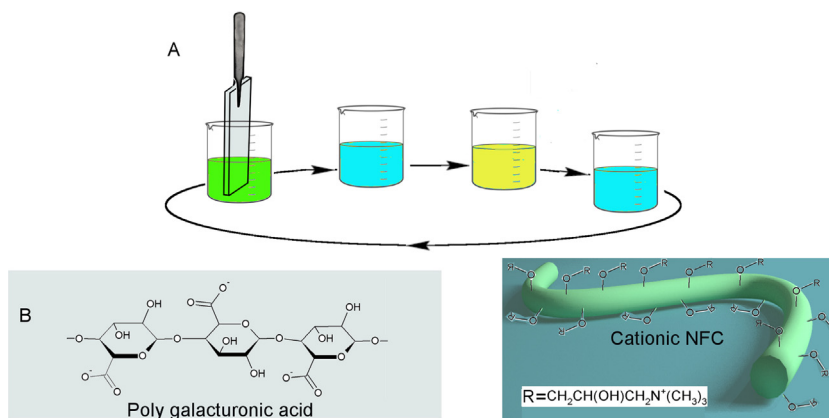
Scheme 1. (a) Schematic image of the layer-by-layer process, (b) the molecular structure of poly(galacturonic acid) and (c) the structure of the cationic NFC.

Gruissem, & Jones, 2000). Pectin has previously been reported to exhibit colon targeting potential, since human microbiota responsible for its break-down is present first in the colon (Martens et al., 2011).

In the present study, the LbL method was employed to build coatings based on cationic NFC and the anionic poly(galacturonic acid) (polyGalA), for chemical structure schematics see Scheme 1b. The coating is bio-inspired since natural types of multilayer structure consisting of pectin and cellulose nanofiber (microfibrils) are abundant in nature, e.g. the so-called primary cell wall (parenchyma cells) found in soft tissue in fruit and vegetables (Buchanan et al., 2000). The development of such coatings could potentially allow microencapsulation of active components both in drug and food applications. Here, we demonstrate the build-up of a bio-inspired ("plant-cell-like") multilayer coating of pectin and NFC. Further we assess the oxygen barrier properties, which are important during storage to increase the oxidative stability of sensitive ingredients, and the environment responsive release properties of the coating. More specifically, the multilayer coatings were tested for simulated environmental stresses such as acidity and bacterial enzyme degradation in the human gut that potentially hydrolyse the coating, thus providing a unique system for the selective release of active components (e.g. drugs, probiotics, peptides) in the gut (Zhu, Gao, Wu, & Qin, 2013).

2. Experimental part

The experimental section can be found in the Supporting information.

3. Results and discussion

3.1. Build-up the multilayer coating

The LbL coating were produced by submerging a negatively charged silica wafer or a Poly(lactic acid) (PLA) film in successive solutions containing either the cationic NFC (0.01 wt%) or the anionic polyGalA (0.1 wt%) for 15 min, as depicted in Scheme 1. The rinsing steps with pure water in between each of these solutions minimized contamination of the next solution. The average optical thickness of the (dry) coating after each bilayer/cycle (one layer cationic NFC and one layer polyGalA) in the growth process was evaluated by spectroscopic ellipsometry (SE), see results in Fig. 1a and b. The results showed a successful build-up of LbL coating. From the raw SE data, Fig. 1a, there was a significant change in both ellipsometry functions during each growth cycle suggesting that more and more material is deposited with each cycle.

The data was fitted using a transparent Cauchy model (see Supporting information for details on the measurements) to give the total average thickness as a function of deposited bilayers, see Fig. 1b. The thickness of each LbL was measured at five different positions on each sample in order to account for possible lateral heterogeneity in the sample. For the first cycle, the total thickness was 2 ± 1 nm. Increasing the incubation time on each solution to 60 min did not significantly affect the coating thickness (Supporting information Fig. S1). The diameter of a single NFC fiber, as determined by height analysis of atomic force microscopy (AFM) images, is 5 ± 1 nm and the fiber length was up to several μm, see Supporting information Fig. S2. The SE thickness is an optical thickness and thus measures an average of the coating thickness. Thus, the SE thickness tends to underestimate the total thickness of the film for heterogeneous films. The total thickness increases with the number of cycles in a linear manner having a 2.61 ± 0.06 nm dependency on the number of LbL. Moreover, the adsorbed amount also presented a linear growth with the number of LbL (see Supporting information, Fig. S3) for which typical refractive index values were obtained using the chosen fitting model (Bergström, Stemme, Dahlfors, Arwin, & Ödberg, 1999). Thus, besides interlayer diffusion (or filling the gaps in the initial coating) there is further binding on the top of the surface leading to film growth.

The topology of the resulting coatings was assessed with tapping mode AFM in air. In Fig. 1c the topology of the coating after 10 LbL is presented. The AFM images show a dense film that is quite heterogeneous in nature, where the individual NFC fibers can be clearly observed (a close-up is shown in Fig. 2a for 8 LbL). The presence of pores in between NFC supports the hypothesis of interlayer diffusion (or filling the gaps in the initial coating) taking place during LbL deposition. Moreover, linear growth is supported by AFM images since the thickness of the 10 LbL coating could be measured ($\sim$100 nm) taking advantage of a defect we found on this particular film (Fig. 1c, inset in Fig. 1b). This value is almost 3 times the calculated using SE. The apparent discrepancy between these values could arise from the heterogeneous character of this film, as previously discussed.

3.2. Resistance of the LbL coating to stresses present in the GI tract

The stomach fluid consists mostly of pepsin, HCl and NaCl. This environment kills bacteria to prevent infections in the digestive system and moreover the acid gives the right pH for the reaction of the protease pepsin. We subjected our coated Si wafers to a simulated gastric fluid (2 g l^{-1} NaCl, 3.2 g l^{-1} pepsin and 0.3% HCl) under stirring for 3 h at 37 °C, and the total ellipsometry thickness and surface topology was characterized with SE and AFM, respectively.
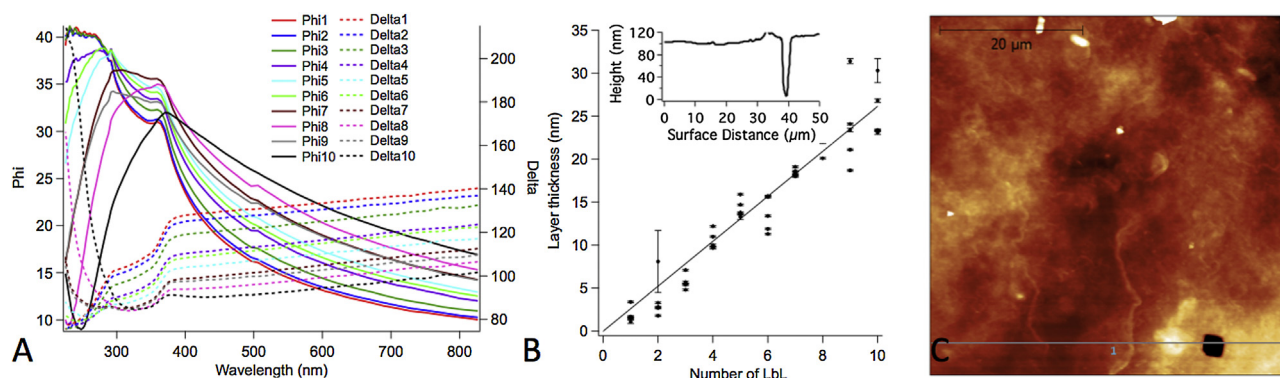
Fig. 1. (a) The raw data from spectroscopic ellipsometry (SE) where the different full (psi function) and broken (delta function) lines represent increasing numbers of bilayers. (b) The evolution of the total thickness of the coating as a function of increasing numbers of bilayers. The coatings were dried prior to measurements. The data in (b) is obtained from spectroscopic ellipsometry results in (a). (c) AFM image of a 10 bilayer coating, showing a hole. The depth of the hole, ~100 nm, is given in the inset image in (b).

No major differences were observed in either the thickness or the morphology of the surface—compare the changes in SE thickness in Fig. 2d and AFM images in Fig. 2a and b. Therefore, the coating seems to survive the chemical and physical stresses in the stomach. The pH of this solution remained constant at a value ~2 during the whole length of the experiments.

Once reaching the gut, the food is exposed to a rich flora that includes between 300 and 1000 different microorganisms and their levels can reach a total population as high as 10^{13}–10^{14} cells (Zhu et al., 2013), which is essential for human well-being. Some of these microorganisms produce enzymes that can degrade pectins including polyGalA (Martens et al., 2011). To simulate the action of the microbiota enzymatic action in the gut, a pectinase enzyme was used at various concentrations (1, 5 and 20 U ml^{-1}) to determine whether the coating was degraded under any of these conditions. SE shows that the layer thickness decreases by 40–50% once the enzyme concentration was raised to 5–20 U ml^{-1} during 3 h (Fig. 2d). Since the pectinase can only degraded the polyGalA and not cellulose, the SE value suggests the partial collapse of the film structure and/or more porous structure of the cellulose based coating. AFM images, however, showed only a small change in the overall morphology of the film: The nanofibers seemed more "swollen" and small aggregates or "particles" appeared on the coating, compare Fig. 2a and c. Also, the roughness (Supporting information, Fig. S4) increased and the apparent height profile (inset Fig. 2) broadened and shifted to higher values once the samples were exposed to the bacterial enzyme solution. The change in both the roughness and apparent height before and after the sample was exposed to the enzyme solution can be caused by the enzymes creating holes in the coating, although irreversible adsorption of enzymes to the coating cannot be disregarded.

3.3. Oxygen barrier properties

The oxygen protective properties of the multilayer coatings were also assessed. In this case, a PLA substrate was coated with 20 LbL on each side (total thickness of coating was estimated to be 249.6 nm based on SE) and measured at 20% relative humidity and 23 °C giving a value of 0.033 ml (STP) mm m^{-2} day^{-1} atm^{-1} for the coating. The oxygen permeability coefficient (OP) for the coating is comparable to that of EVOH (Aulin et al., 2010), which is typically used in high oxygen barrier protection applications. However, from a sustainability point of view, our coating is more attractive since it could potentially be a direct part of the edible system, minimizing the amount of waste. A neat cationic NFC film has an OP value of 0.016 ml (STP) mm m^{-2} day^{-1} atm^{-1} at 20% RH and 23 °C. Pectin films have a reported OP of 17.4 ml (STP) mm m^{-2} day^{-1} atm^{-1} at 55% RH and 23 °C (de Moura, Aouada, Zucolotto, & Mattoso, 2011). Note that herein, the measurements were performed at 20% relative humidity, and the OP of a neat pectin film will be lower at this relative humidity, as expected given the known effect of water on barrier properties of pectin films (Vartiainen, Tammelin, Pere, Tapper, & Harlin, 2010).

The oxygen permeability was also measured after the simulated gastric fluid and bacterial enzyme treatment. In this case, the oxygen permeability of the coating and substrate was very close to the value of the neat PLA substrate itself, suggesting very little contribution from the coating to the oxygen barrier properties. This
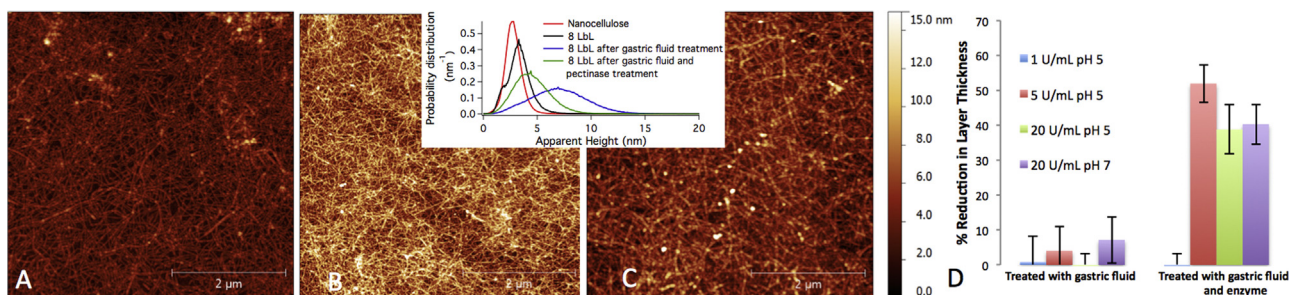

Fig. 2. (a) AFM image of the 8 LbL coating. The same surface after exposure to (b) simulated gastric fluid (3 h, 2 g l^{-1} NaCl, 3.2 g l^{-1} pepsin and 0.3% HCl) and in (c) simulated stomach conditions and pectinase exposure (3 h of enzyme solution). The inset shows the apparent height distributions for the 8 LbL coating before treatment, after treatment with simulated gastric fluid and treatment with gastric fluid/pectinase. (d) The reduction of the total coating thickness after each treatment (gastric fluid or gastric fluid/enzyme).

could suggest that the coating was partially or completely decoupled from the PLA substrate under the exposure to the simulated gastric fluid and the pectinase solution. One explanation to this could be that the adhesion of the LbL-coating to the PLA substrate was probably not as strong as that to the silica wafer.

4. Conclusions

Spectroscopic ellipsometry, atomic force microscopy and oxygen permeability results showed successful buildup of a multilayer coating based on cationic nanofibrillated cellulose and polygalacturonic acid. The multilayer coating is dense and thick and presents low permeability to oxygen ($0.033 \, \mathrm{ml \, (STP) \, mm \, m^{-2} \, day^{-1} \, atm^{-1}}$), typically in the same order of magnitude as for ethylene vinyl alcohol films. Moreover, the coating is able to survive in simulated gastric fluid and it is partially degraded (polygalacturonic acid) upon exposure to pectinase enzyme, which simulate the action of the microbial symbionts present in the human gut. After this exposure, the permeability to oxygen has increased, which strengthens the conclusions that the coating has been partially degraded. Such coatings could potentially be used for targeted release of active components (e.g. drugs, probiotics, peptides) in the human colon.

Acknowledgements

Appendix A. Supplementary data

Supplementary data associated with this article can be found, in the online version, at http://dx.doi.org/10.1016/j.carbpol.2014.08.011.

References

Aulin, C., Gallstedt, M., & Lindstrom, T. (2010). *Cellulose, 17,* 559.
Bergström, L., Stemme, S., Dahlfors, T., Arwin, H., & Ödberg, L. (1999). *Cellulose, 6,* 1.
Buchanan, B. B., Gruissem, W., & Jones, R. L. (2000). *Biochemistry & molecular biology of plants.* Rockville, MD., Great Britain: American Society of Plant Physiologists.
de Moura, M. R., Aouada, F. A., Zucolotto, V., & Mattoso, L. H. C. (2011). *Polymer-Plastics Technology and Engineering, 50,* 1323.
Dubas, S. T., Kumlangdudsana, P., & Potiyaraj, P. (2006). *Colloids and Surfaces A: Physicochemical and Engineering Aspects, 289,* 105.
Eichhorn, S. J., Dufresne, A., Aranguren, M., Marcovich, N. E., Capadona, J. R., Rowan, S. J., et al. (2010). *Journal of Materials Science, 45,* 1.
Kim, J. H., Kim, S. H., & Shiratori, S. (2004). *Sensors and Actuators B: Chemical, 102,* 241.
Li, Y. C., Schulz, J., Mannen, S., Delhom, C., Condon, B., Chang, S., et al. (2010). *ACS Nano, 4,* 3325.
Martens, E. C., Lowe, E. C., Chiang, H., Pudlo, N. A., Wu, M., McNulty, N. P., et al. (2011). *PLoS Biology, 9.*
Priolo, M. A., Gamboa, D., Holder, K. M., & Grunlan, J. C. (2010). *Nano Letters, 10,* 4970.
Saito, T., Kuramae, R., Wohlert, J., Berglund, L. A., & Isogai, A. (2013). *Biomacromolecules, 14,* 248.
Sukhishvili, S. A. (2005). *Current Opinion in Colloid & Interface Science, 10,* 37.
Svagan, A. J., Akesson, A., Cardenas, M., Bulut, S., Knudsen, J. C., Risbo, J., et al. (2012). *Biomacromolecules, 13,* 397.
Vartiainen, J., Tammelin, T., Pere, J., Tapper, U., & Harlin, A. (2010). *Carbohydrate Polymers, 82,* 989.
Westwood, M., Roberts, D., & Parker, R. (2011). *Carbohydrate Polymers, 84,* 960.
Westwood, M., Noel, T. R., & Parker, R. (2013). *Carbohydrate Polymers, 94,* 137.
Wood, K. C., Boedicker, J. Q., Lynn, D. M., & Hammond, P. T. (2005). *Langmuir, 21,* 1603.
Zhu, Q. C., Gao, R. Y., Wu, W., & Qin, H. L. (2013). *Tumor Biology, 34,* 1285.